The depth dependence of earthquake duration and implications for rupture mechanisms

John E. Vidale* & Heidi Houston†

* MS 977, US Geological Survey, 345 Middlefield Road, Menlo Park, California 94025, USA
† Institute of Tectonics, Earth Sciences Board, University of California, Santa Cruz, California 95064, USA

THE duration of rupture is a fundamental characteristic of earthquakes, and is important for understanding the mechanics of faulting[1,2]. The complexity of the seismic source and the incoherence of the high-frequency seismic wavefield often inhibit the identification, location and timing of features in the later part of earthquake rupture. Here we sum many teleseismic records from regional seismic arrays, producing an unusually clear depiction of the earthquake source at short periods by suppressing background noise and coda generated near the receivers. The ending, as well as the beginning, of rupture is clearly identifiable for most earthquakes examined. Measurements of 130 large earthquakes show that near 100 km depth, rupture duration averages 11 s when scaled to a moment of 10^{26} dyn cm; this decreases to 5.5 s at 650 km depth. Models of faulting suggest that duration should be inversely proportional to the shear-wave velocity and the cube root of stress drop. Thus, to explain the observed twofold decrease in duration with depth, stress drops would have to increase by a factor of four, as shear velocity increases with depth by only about 20%. However, observed stress drops show no strong trend with depth[3,4], suggesting that the faulting process changes with depth.

We have collected teleseismic recordings of 162 earthquakes for this study, across the Northern California Seismic Network, the Southern California Seismic Network and the University of Washington Seismic Network. The networks each have several hundred short-period vertical-component seismometers that are used primarily to study regional seismicity and tectonics[5].

From April 1980 to June 1992 there were 169 earthquakes in the distance range from 35–90° from California, larger than 1.6×10^{25} dyn cm in moment and more than 100 km in depth. The chosen distance range ensures that little distortion in the waveform results from propagation through the mantle, the moment range ensures that there is sufficient duration of rupture to measure reliably, and the depth range ensures that reflections from the surface above the earthquake (pP and sP) arrive later than the end of the direct waves.

As the aperture of each network spans several hundred kilometres and the earthquakes are 3,000–10,000 km distant, each station should see similar P-wave arrivals from a given earthquake. However, crustal structure, which is different for each station, produces a tail of scattered waves after the direct P wave that distorts and obscures the later part of each arrival.

We then isolate the component of the P arrival that is common to all stations. First, records from the stations with high noise levels or anomalously strong scattered coda are eliminated. This leaves 50–200 clean seismograms for each event. Next, these traces are aligned by eye on an easily identified feature in the first second or two of the P-wave arrival. Finally, the traces are normalized to a peak amplitude of unity and added together.

As the scattered energy is incoherent between stations, in the stacked trace it is diminished by a factor of $\sqrt{N}$ where N is the number of traces stacked. Thus, we recover the direct arrivals by cancelling the scattered coda. Although coda scattered within tens of kilometres of the source contributes to our stacked trace, its amplitude is expected to be small. The abrupt termination of most of the stacked traces confirms that near-source scattering usually does not obscure the observation of end of the source.

The effectiveness of this procedure is demonstrated by Fig. 1*a*, which shows the sum of 69 short-period traces for a deep earthquake under Argentina. From the P-wave stack shown in Fig. 1*a*, the beginning and end of the rupture may be reliably identified at 9.5 and 15.5 s. The rupture duration is 6 s. More examples are shown in Fig. 1*b*.

For completeness, we note that 39 of the 169 events meeting our selection criterion were not used. P waves from 24 of these events were too near a node in the radiation pattern to allow reliable identification of the end of the rupture. Events are considered too nodal if the P radiation coefficient, which is calculated from the Harvard Moment Tensor mechanism, is less than 0.1. Two events showed two episodes of faulting, separated by 5–10 s of quiescence. Six earthquakes, all in the depth range 100–350 km, are omitted because the end of rupture is difficult to identify. Seven events did not trigger any of the three arrays,

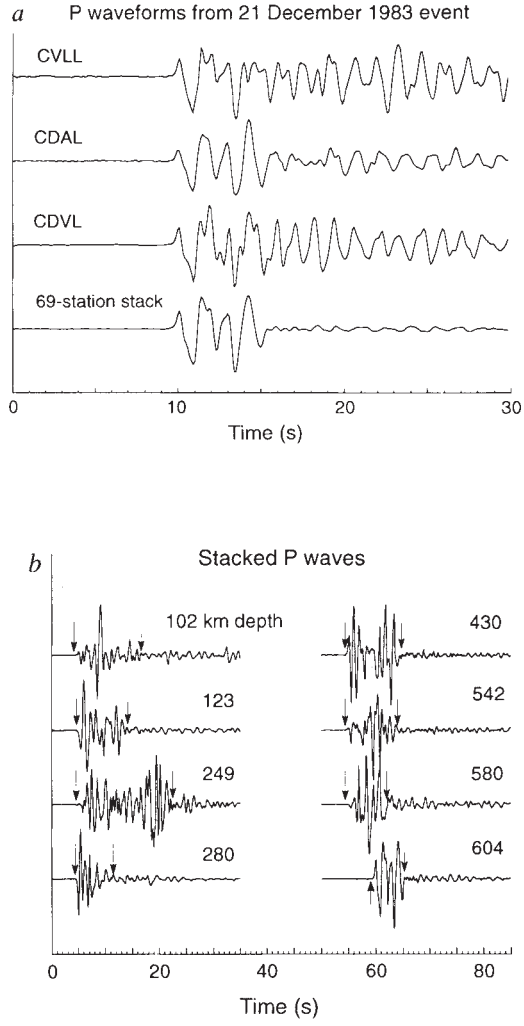

FIG. 1 *a*, An example of the stacking process. The top three traces are short-period vertical-component seismograms from the stations CVLL, CDAL and CDVL in the Northern California Seismic Network. The bottom trace is the sum (or stack) of 69 high-quality traces, selected from the 400 stations of the network, on the basis of low background noise, small near-surface reverberations and the absence of clipping. Note the well defined ending of the short-period P-wave radiation. *b*, Eight stacks of earthquakes with moments in the range $1.7–3.2 \times 10^{26}$ dyn cm. The arrows indicate the inferred start and end of each rupture. The depth of the events are given. The origin times of the traces are arbitrary.

suggesting these events produced weak and perhaps protracted short-period waves.

Figure 2 shows the durations of the remaining 130 events. Larger earthquakes have a longer duration, as expected, because the rupture length is greater. Deeper earthquakes generally rupture more rapidly than shallow and intermediate events. As earthquake duration is proportional to the linear dimension of the fault, which in turn is proportional to the cube root of moment[6], we scale the durations to a moment of 10^{26} dyn cm and compare scaled durations with depth in Fig. 3. The tendency for the durations of the deeper events to be shorter is clear. The intermediate and shallow events show more variation in scaled duration than do the deep events.

This study contains many more duration measurements than previous studies, and the durations are measured with greater accuracy. Figure 3 indicates an average scaled duration of 11 s for events with 10^{26} dyn cm moment at 100 km depth, decreasing to 5.5 s for events near 670 km depth. It has also been shown that rise times are about twice as fast for deep earthquakes as for intermediate depth events[3]. Our present work shows that not only the initiation, but the entire rupture process is faster for deep earthquakes by roughly the same amount.

Previous studies, predominantly of shallow earthquakes, found average durations of 12 s (ref. 7) and 10.2 s (refs 8, 9), which are consistent with our estimates. Our durations are also generally consistent with previous duration estimates for deep earthquakes[10–13]. The studies may differ because previous long-period estimates fit the duration of the largest long-period pulse, whereas our short-period stacks can clearly show the beginning and ending of short-period radiation from the source. The use of inaccurate Green's functions to model shallow earthquakes can make some of the previous estimates too long[14]. Taken together, the other studies show considerable scatter, which may result from the different methodologies used in each study.

A limitation of our data is that it samples seismic radiation in essentially only one direction from the source. If the rupture proceeds unilaterally directly towards or away from the ray path to the array, then the measured durations could be significantly shortened or lengthened, respectively. This phenomenon is termed directivity. However, inversions for the slip distributions in deep earthquakes suggest that their rupture is generally not purely unilateral[12]. Moreover, we found no dependence of scaled duration on subduction zone. Accordingly, it appears that our measured durations are not severely affected by directivity.

The observation of high-frequency seismic radiation throughout the entire rupture duration coupled with the good agreement with more broad-band duration estimates suggests that significant slow afterslip is not a general feature of moderately large earthquakes. Similarly, the sharp initiation of each event precludes more than about 1 to 2 s of accelerating slow slip at the start. Our sensitivity is limited to frequencies between 0.2 and 2 Hz, however.

We would expect some decrease in the duration of earthquakes with depth solely because the shear velocity increases with depth, leading to faster expansion of the rupture front. To explore such effects, consider a circular crack model. The seismic moment is given by

$$M_0 = \mu \pi r^2 D$$

where μ is the shear modulus, D is the average fault slip, and r is the radius of the fault area. The static stress drop during an earthquake is proportional to the displacement divided by a fault dimension[6]:

$$\Delta\sigma \propto \frac{\mu \pi D}{r} = \frac{M_0}{r^3}$$

Therefore

$$r \propto \left(\frac{M_0}{\Delta\sigma}\right)^{1/3}$$

and duration τ

$$\tau \propto \frac{r}{v_s} \propto \frac{M_0^{1/3}}{v_s \Delta\sigma^{1/3}}$$

assuming that rupture velocity is proportional to the shear wave velocity v_s. Thus, scaled durations would be expected to follow

$$\frac{\tau}{M_0^{1/3}} \propto \frac{1}{v_s \Delta\sigma^{1/3}}$$

Therefore, for this model to explain the observed decrease in scaled durations with depth of a factor of two from 100 to 670 km, stress drops would have to increase with depth by a factor of four as v_s increases by only 20% over this depth range. Observed stress drops, however, show no such dramatic increase according to a review of eight studies[4], as well as ref. 3, which is discussed below.

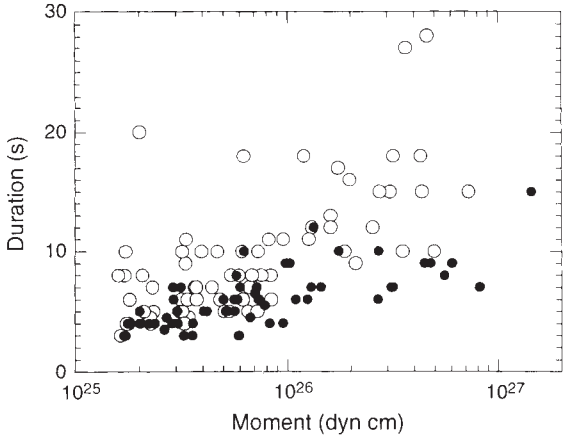

FIG. 2 Seismic moment is plotted against the earthquake duration measured from short-period stacks, as illustrated in Fig. 1. Duration increases as the cube root of moment, as predicted by source scaling relations[6]. Moments are from the Harvard Centroid Moment Tensor catalogue[22]. ○, Depth < 350 km; ●, depth > 350 km.

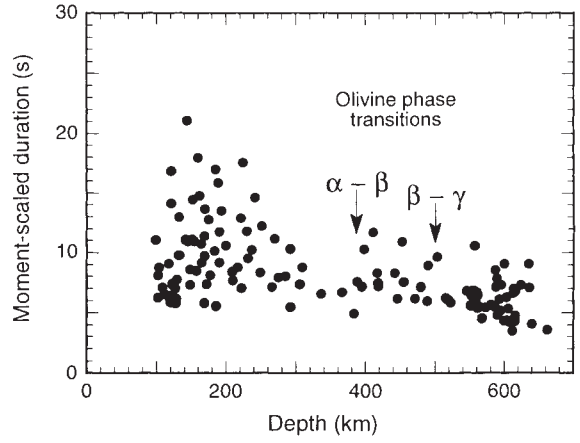

FIG. 3 Moment-scaled duration plotted against depth. The scaled duration is obtained by dividing the duration shown in Fig. 2 by the cube root of moment, normalized to 10^{26} dyn cm. The decrease in duration with depth is greater than that expected from source scaling relations, which predict that duration should be proportional to the inverse of the shear-wave velocity.

Stress drops are difficult to measure and have been estimated by several methods, including using durations measured from pulse widths, as mentioned above[13,15]. Stress drop and duration, although related, are fundamentally different physical properties. It is possible for an event to have both high stress drop and long duration or low stress drop and short duration, depending on the detailed shape of the source time function, or equivalently, the source spectrum. One problem with using duration to estimate stress drops, besides the measurement difficulty mentioned above, is that it uses essentially only one part of the source spectrum, the corner frequency. An independent way of measuring stress drop that uses the entire bandwidth of the source spectrum was applied to 68 intermediate and deep earthquakes[3]. In this work, seismically-radiated energies were estimated from the squared velocity-source spectrum of broadband teleseismic body waves recorded by the Global Digital Seismic Network (GDSN). From the ratio of energy to moment, an Orowan stress drop can be calculated[16]. These stress drops were found to be constant with depth[3].

Therefore, our observation of durations decreasing by a factor of two, while the Orowan stress drop remains constant with depth, requires that some element of rupture changes with depth be incorporated into the above model. Why might earthquake rise time and duration depend on depth? The fault geometry could become less elongated and more equi-dimensional with depth. Alternatively, faulting at shallower depths may be more episodic or non-steady, perhaps because of the greater heterogeneity in temperature and composition that is present nearer the surface of the Earth. These two explanations may be related; elongated ruptures may be more intermittent, whereas equi-dimensional faulting might spread out more smoothly as the rupture develops. It is also possible that the rupture velocity is increasing faster with depth than the shear-wave velocity. The observed decrease in duration with depth, together with a constant stress drop, suggests a change in the shape of the source spectrum. Specifically, intermediate depth events would need to have more high-frequency energy (radiation at periods shorter than the earthquake duration) and deep events less such energy.

These rupture properties, in turn, may be influenced by a transition from frictional faulting to transformational faulting at intermediate depths[17,18]. They could also be influenced by the transition from α-olivine to β-phase near 390 km depth, the transition from β-phase to γ-phase near 500 km depth, or other phase transitions within subducting slabs[19]. The depths above are appropriate for temperatures within a cold slab[20], and the α to β conversion depth in slabs is supported by seismic measurements[21]. These depths also correspond to the minima in the frequency of earthquakes visible in Fig. 3.

The depth dependence of the durations shown in Fig. 3 suggests that phase transitions may be influential. Events in the α-olivine stability field show the largest variation in duration. Events in the β-phase region have more moderate variations, and the events in the γ-phase region, which are the shortest duration events, show the least variation in duration. □

Received 15 March; accepted 9 July 1993.

1. Kanamori, H. A. *Rev. Earth planet. Sci.* **14,** 293–322 (1986).
2. Wald, D. J. thesis, California Inst. Technol., Pasadena (1992).
3. Houston, H. & Williams, Q. *Nature* **352,** 520–522 (1991).
4. Frohlich, C. *Rev. Earth planet. Sci.* **17,** 227–254 (1989).
5. Benz, H. M., Vidale, J. E. & Mori, J. *EOS* (submitted).
6. Kanamori, H. & Anderson, D. L. *Bull. seism. Soc. Am.* **65,** 1059–1072 (1975).
7. Kanamori, H. & Given, J. W. *Phys. Earth planet. Inter.* **27,** 8–31 (1981).
8. Ekström, G. thesis, Harvard Univ. (1987).
9. Ekström, G. & Engdahl, E. R. *J. geophys. Res.* **94,** 15499–15520 (1989).
10. Kuge, K. *J. geophys. Res.* (in the press).
11. Glennon, M. A. & Chen, W.-P. *J. geophys. Res.* **98,** 735–769 (1992).
12. Fukao, Y. & Kikuchi, M. *Tectonophysics* **144,** 249–269 (1987).
13. Chung, W. & Kanamori, H. *Phys. Earth planet. Inter.* **23,** 134–159 (1980).
14. Wiens, D. A. *J. geophys. Res.* **94,** 2955–2972 (1989).
15. Mikumo, T. *J. Phys. Earth* **19,** 303–320 (1971).
16. Houston, H. *Geophys. Res. Lett.* **17,** 1021–1024 (1990).
17. Green, H. W. & Burnley, P. C. *Nature* **341,** 733–737 (1989).
18. Kirby, S. H. *J. geophys. Res.* **92,** 13789–13800 (1987).
19. Anderson, D. L. & Bass, J. D. *Nature* **320,** 321–328 (1986).
20. Ito, E. & Takahashi, E. *J. geophys. Res.* **94,** 10637–10646 (1989).
21. Vidale, J. E. & Benz, H. M. *Nature* **356,** 678–683 (1992).
22. Dziewonski, A. M. & Woodhouse, J. H. *J. geophys. Res.* **88,** 3247–3271 (1983).

ACKNOWLEDGEMENTS. We thank R. Stein, C. Ammon, A. McGarr, C. Frohlich and Q. Williams for discussions. H. Benz, R. Benson and K. Douglas helped in procuring network data. We thank K. Kuge for preprints. Partial support for this work was provided by the National Science Foundation, the W. M. Keck Foundation, the Institute of Tectonics and the C. F. Richter Laboratory, University of California, Santa Cruz (H.H.).

Magnetite formation by a sulphate-reducing bacterium

Toshifumi Sakaguchi, J. Grant Burgess & Tadashi Matsunaga*

Department of Biotechnology, Tokyo University of Agriculture and Technology, Koganei, Tokyo 184, Japan

BACTERIAL production of magnetite (Fe_3O_4)[1] makes an important contribution to iron biomineralization and remanent magnetization of sediments[2,3]. Accurate magnetostratigraphy, reconstruction of the Earth's past magnetic-field behaviour and extraction of environmental information from the geomagnetic record depend on an understanding of the conditions under which bacterial magnetite is formed. In aquatic sediments, the process is thought to be restricted to a zone between the levels at which nitrate and iron reduction occur[4]. In sulphate-reducing habitats, deeper in the sediment, the presence of H_2S reduces iron oxyhydroxides to iron sulphides[5,6]. Thus magnetite would not be expected to form under such reducing conditions[5,7]. We report here the isolation and pure culture of a dissimilatory sulphate-reducing bacterium, designated RS-1, which can synthesize intracellular magnetite particles. RS-1 is a freshwater anaerobe which is also capable of extracellular iron sulphide precipitation. This isolate illustrates the wider metabolic diversity of magnetic bacteria and suggests the presence of a novel mechanism of magnetic biomineralization. The discovery of such bacteria may also explain why large quantities of magnetite have been observed in sulphate-rich, oil-bearing, sedimentary deposits[8–11]. In addition, these results significantly enlarge the environments in which biogenic magnetite may be expected to occur and have important implications regarding the evolution of the ability to synthesize magnetite.

Freshwater sulphide-rich mud was collected from a waterway near Kameno river, Wakayama prefecture, in western Japan. Samples were allowed to enrich for 2 weeks in 1-l glass containers. Magnetic bacteria were not observed in water from these enrichments. Samples of the water were inoculated anaerobically into a modified isolation medium[12]. One week later, a Gram-negative magnetic bacterium, designated RS-1, was isolated in pure culture by restreaking single colonies onto isolation-medium agar plates. Cells were 3–5 μm in length with a diameter of 0.9–1.5 μm, with a helicoid to rod shaped morphology and a single polar flagellum (Fig. 1*a*). The guanine plus cytosine content of purified genomic DNA was 65.8 ± 0.2 M per cent, as determined by HPLC. Additional morphological characteristics differed from those of previously cultured magnetic bacteria[12–18]. Although RS-1 cells oriented and swam along magnetic-field lines (magnetotaxis) (Fig. 1*b*), they showed stronger anaerotaxis and accumulated at an anaerobic zone in the centre of a slide preparation with artificial magnetic fields. Individual cells could reverse their swimming direction without turning round. The ratio of magnetic north to south seeking cells was 1 : 1 in a population of cultured cells.

Although RS-1 was catalase positive and oxidase negative, it could not be cultured in the presence of oxygen and was a strict anaerobe. RS-1 could only grow in the presence of sulphate:

* To whom correspondence should be addressed.